Lab on a chip

Electronic Supplementary Information

Transdermal on-demand drug delivery based on an iontophoretic hollow microneedle array system

Usanee Detamornrat [†,a], Marc Parrilla [*,†,a,b,c], Juan Domínguez-Robles [a], Qonita Kurnia Anjani [a], Eneko Larrañeta [a], Karolien De Wael [b,c], Ryan F. Donnelly [*,a]

[a] School of Pharmacy, Medical Biology Centre, Queen's University Belfast, 97 Lisburn Road, Belfast BT9 7BL, United Kingdom.

[b] A-Sense Lab, Department of Bioscience Engineering, University of Antwerp, Groenenborgerlaan 171, 2020 Antwerp, Belgium.

[c] NANOlab Center of Excellence, University of Antwerp, Groenenborgerlaan 171, 2020, Antwerp, Belgium

* Corresponding authors

† Shared authorship

Table of contents

Methods employed in the manuscript

Reagents and instrumentation

Agarose, phosphate buffer saline (PBS) tablets (10 mM phosphate buffer, 2.7 mM KCl and 137 mM NaCl pH 7.4), methylene blue (hydrate, ≥95%), fluorescein sodium and BSA-FITC were purchased from Sigma-Aldrich, UK. Lidocaine hydrochloride was purchased from Fagron, UK.

Conductive pastes of silver (Ag) for the anode fabrication and of silver chloride (AgCl) for the cathode fabrication were purchased from Sun Chemicals, UK. 3M 9471LE adhesive transfer tape was used to stick the MNs on the holder.

Neonatal porcine skin was acquired from stillborn piglets and excised immediately (< 24 h post-partum) and trimmed to 500 µm thickness using an electric Integra Padgett® dermatome Model B (Integra Life Sciences Corporation, Ratingen, Germany). The skin was stored at −20 °C until it was needed. The neonatal porcine skin was shaved and equilibrated in PBS (pH 7.4) for 15 min prior to use.

Franz diffusion cells and a heating circulator were purchased from PermeGear (PA, USA). All experiments were performed using 25 mm clear jacketed Franz cells with flat ground joint. The volume of the receptor compartment is 20 mL. Franz diffusion cells were housed within a diffusion drive console that supported magnetic stirring (600 rpm) and temperature regulation (37 ± 1 °C).

Iontophoresis was performed by applying a certain current between the anode and cathode with a Palmsens4 potentiostat (PalmSens, The Netherlands) controlled using PSTrace v5.9 software.

Characterization of the hollow MN array

The mechanical strength of HMNs was evaluated using a TA-TX2 Texture Analyzer (Stable Micro Systems, Haslmere, UK) in a compression mode. The HMN array was attached to the moving test probe of the Texture Analyzer using double-sided adhesive tape (Office Depot, Boca Raton, USA). To assess the insertion depth, Parafilm® M was used as a skin simulant of neonatal porcine skin as described previously.[1] A sheet of Parafilm® M was folded to form an eight-layer film (approximately 1 mm thickness). Subsequently, the HMN array was inserted into the film using the Texture Analyzer, with the probe lowered onto the film at a speed of 1.0 mm s^{-1}, with an exerted force of 32 N per array, and held for 30 s. The HMN array was removed from the film after insertion at a speed of 10.0 mm s^{-1}. The film was then unfolded and the number of holes in each layer of Parafilm® M and the change in needle height were evaluated under the Leica EZ4 D digital microscope. The percentage of holes in each layer relative to the number of MNs on the array was calculated using Equation 1.

$$Holes\ in\ Parafilm^{®}\ M\ layer\ (\%) = \frac{number\ of\ holes\ observed}{number\ of\ MN\ in\ the\ array} \times 100 \quad \text{Eq. 1}$$

The skin insertion study was performed using the excised neonatal porcine skin (600 µm thickness). The skin was placed on top of an eight-layer film and the test was conducted using the same setup as per the insertion test using Parafilm® M layers. Subsequently, the height of

the HMNs and the number of holes in the skin created by the HMNs were measured under the Leica EZ4 D digital microscope.

Fabrication of three-dimensional printed MN holder (3DP MN holder)

In order to use the HMN array for iontophoresis-based drug delivery, the MN holder was required to hold the MN array, contain drug-loaded agarose gel (drug reservoir), and connect to the power supply. Two parts of the MN holder were designed using Shapr3D and printed using a fused deposition modeling (FDM) 3D printer (Ultimaker 3, USA) with a 0.4 mm print core. The material and key printing parameters for 3DP are as follows: polypropylene filament (PP, 2.85 mm diameter, natural, Ultimaker, USA), 100% infill, 0.1 mm layer height, 0.38 mm line width, 205 °C printing temperature, 85 °C build plate temperature, and 25 $mm.s^{-1}$ print speed.

The MN holder consists of a body and a cap. The body part was attached to the HMN array using cyanoacrylate glue and subsequently loaded with a drug-loaded agarose gel. The cap part was mounted with a silver or silver chloride paste and connected to a wire prior to use.

Tables

Table S1. Dimensions of the HMN arrays obtained by the measurement under the optical microscopy. Data of actual dimensions are presented as means ± standard deviations (SD), N = 3.

Parameter	CAD	Resulting HMN arrays	Difference from CAD (%)
	Dimension (μm)	Mean ± SD (μm)	
Height	1000	994 ± 56	0.6
Width	750	736 ± 12	1.9
Tip-to-tip interspacing	2000	2025 ± 45	1.2
Baseplate thickness	300	289 ± 40	3.7
Hole diameter bottom	100	94 ± 7	6.0
Hole diameter on MN body	540	505 ± 24	6.5

Figures

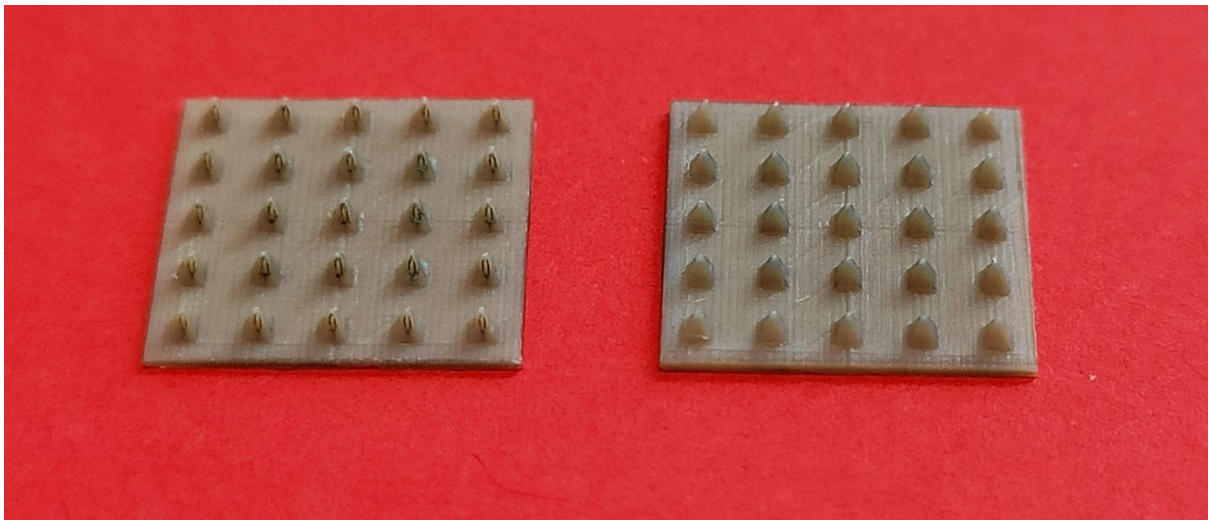

Fig. S1. Image of the HMN arrays made of PEEK.

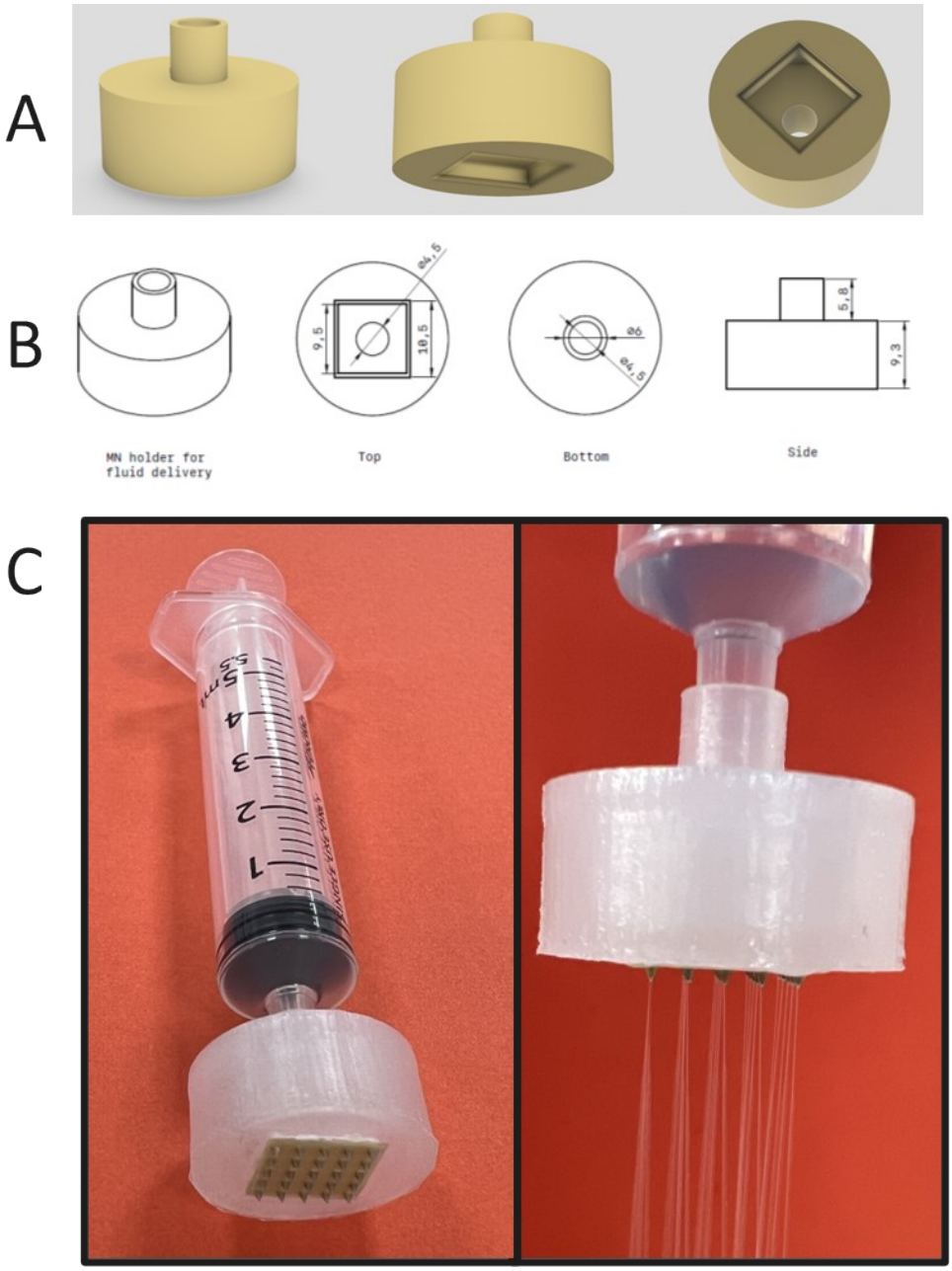

Fig. S2. (A) CAD of the MN holder for fluid delivery, (B) Two-dimensional drawing of the MN holder for fluid delivery at different perspectives. Dimensions are shown in mm unit. (C) The HMN array attached to the MN holder for fluid delivery and the flow of water through the channels of the HMN array.

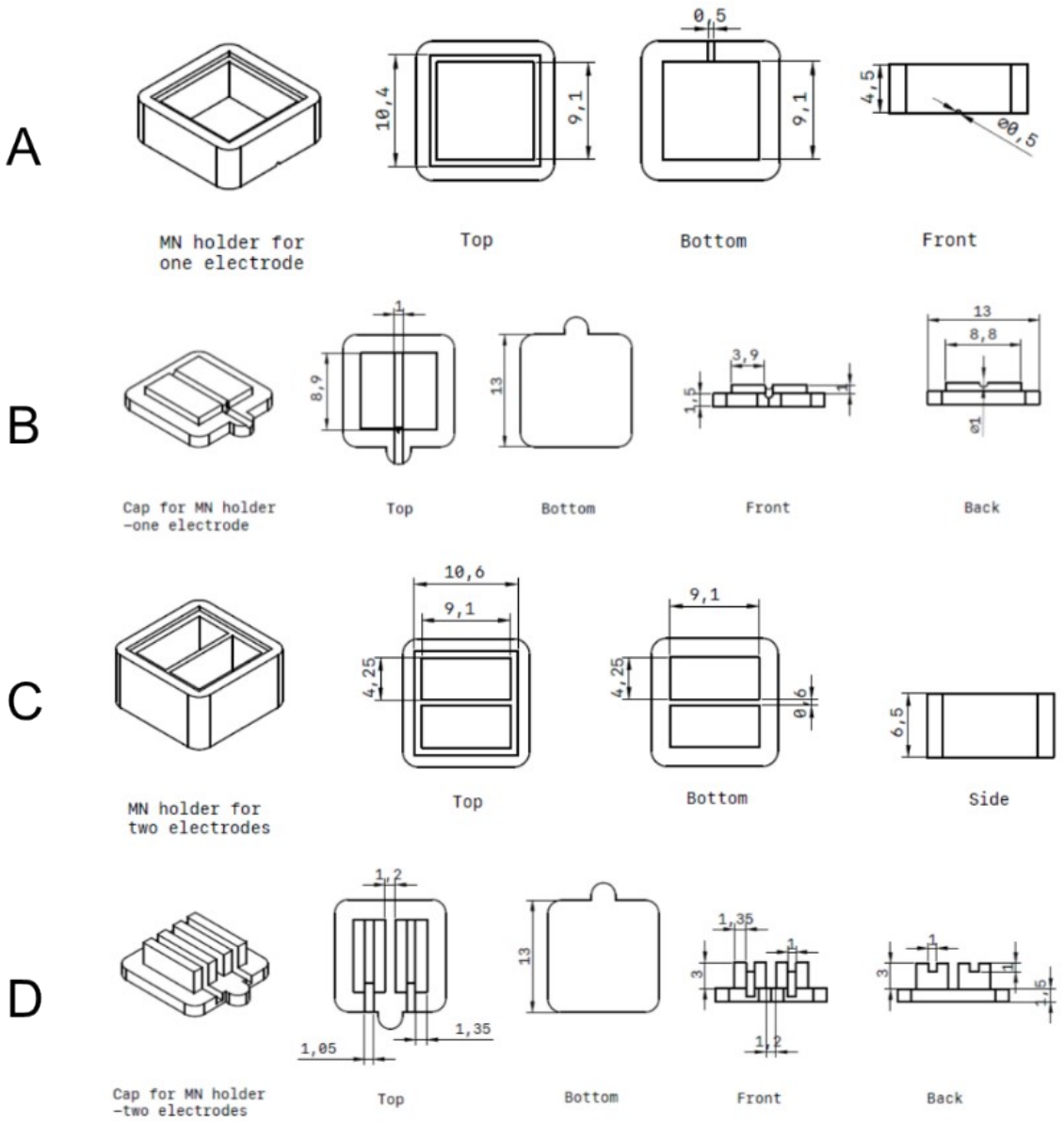

Fig. S3. Drawing of designs at different perspectives: (A) MN holder for one electrode, (B) Cap for the MN holder for one electrode, (C) MN holder for two electrodes, and (D) Cap for the MN holder for two electrodes. The dimensions are shown in mm unit.

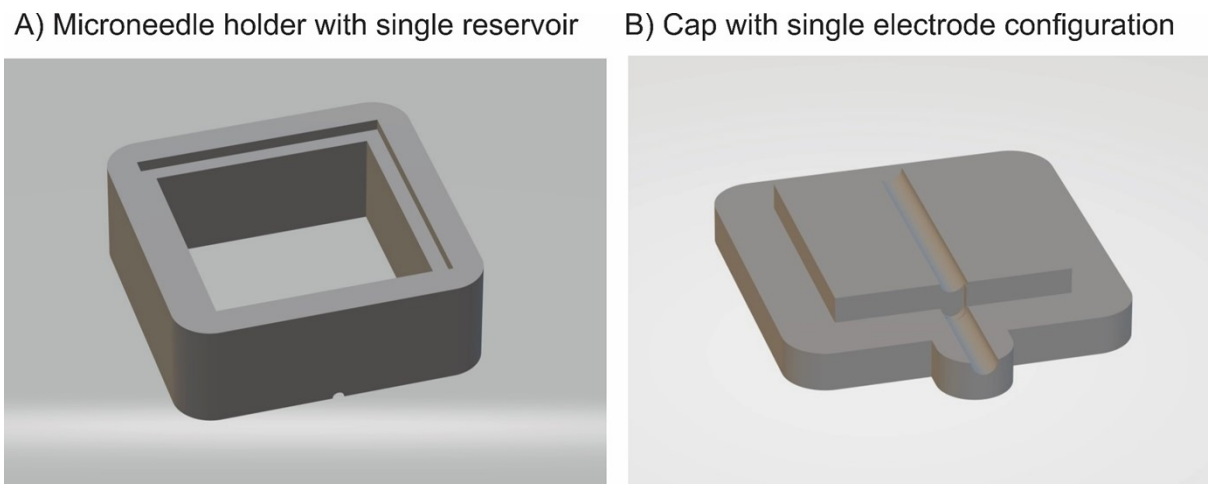

Fig. S4. CAD of the MN holder for single electrode configuration: (A) holder and (B) cap.

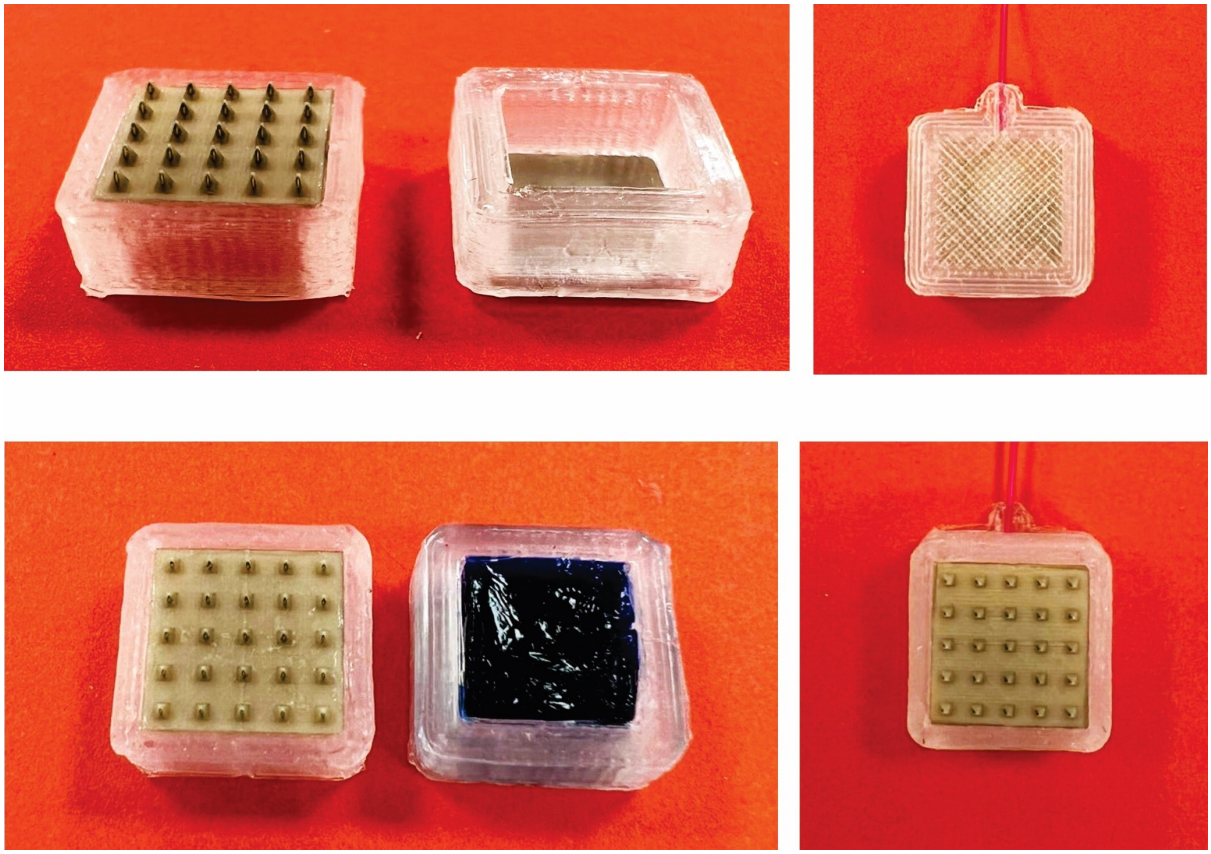

Fig. S5. Images of the assembly of the hollow microneedle iontophoretic system using a single electrode configuration.

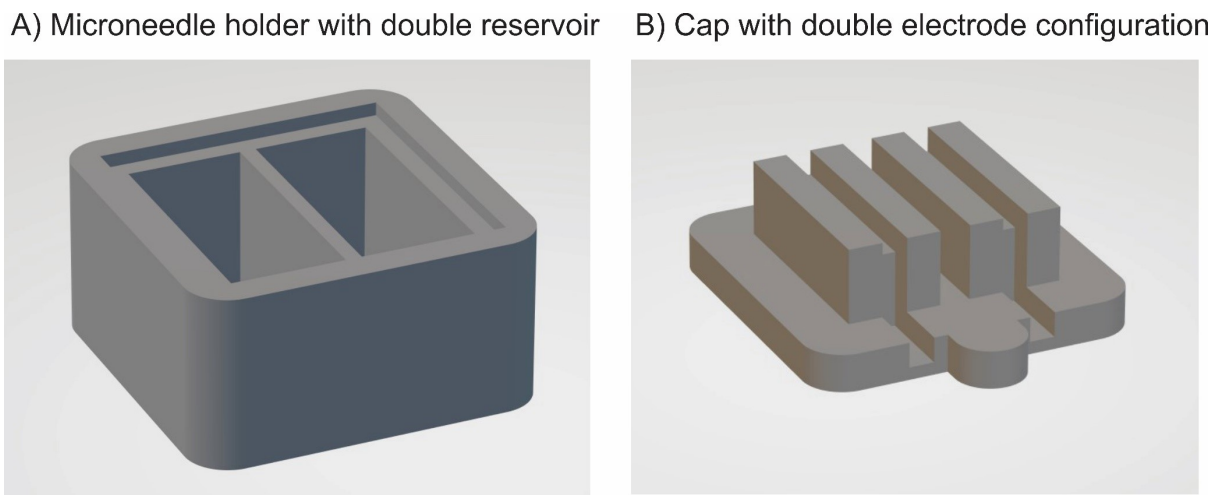

Fig S6. CAD of the MN holder with the double electrode configuration: (A) holder and (B) cap.

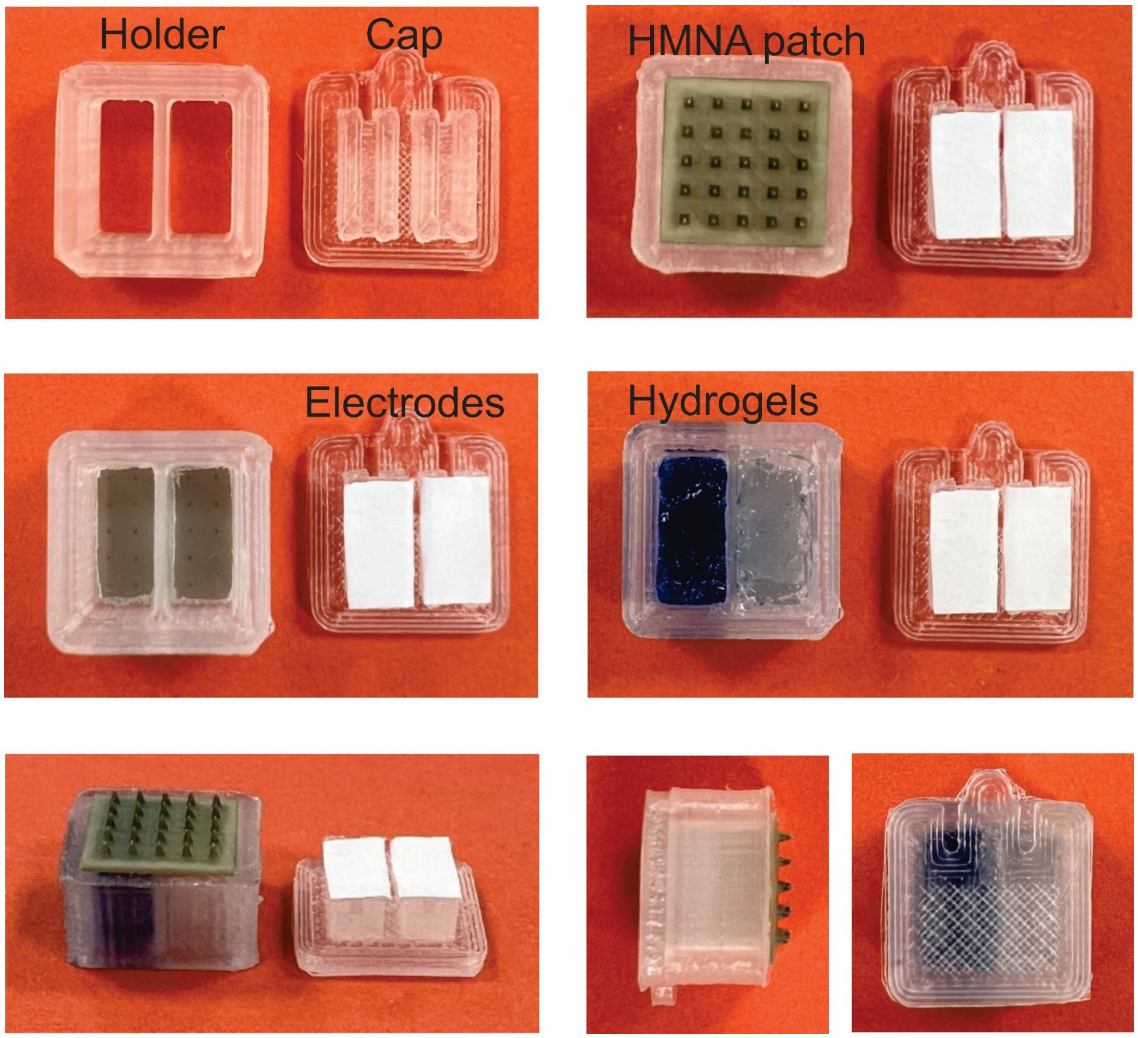

Fig. S7. Images of the assembly of the integrated hollow microneedle iontophoretic system using a two-electrode configuration.

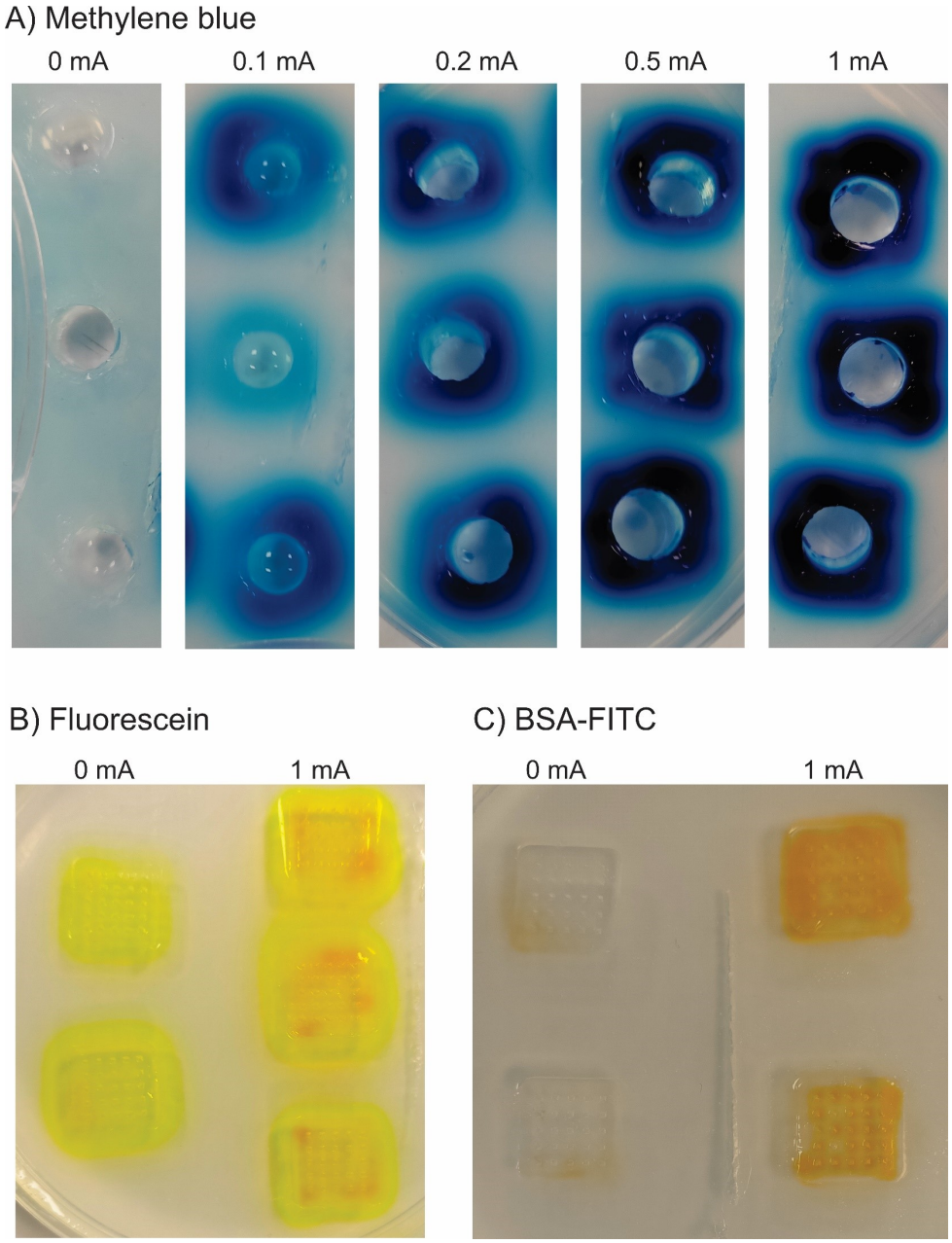

Fig. S8. Image of the agarose gel after the *in vitro* tests using the HMNI device: (A) Methylene blue, (B) Fluorescein sodium, and (C) BSA-FITC.

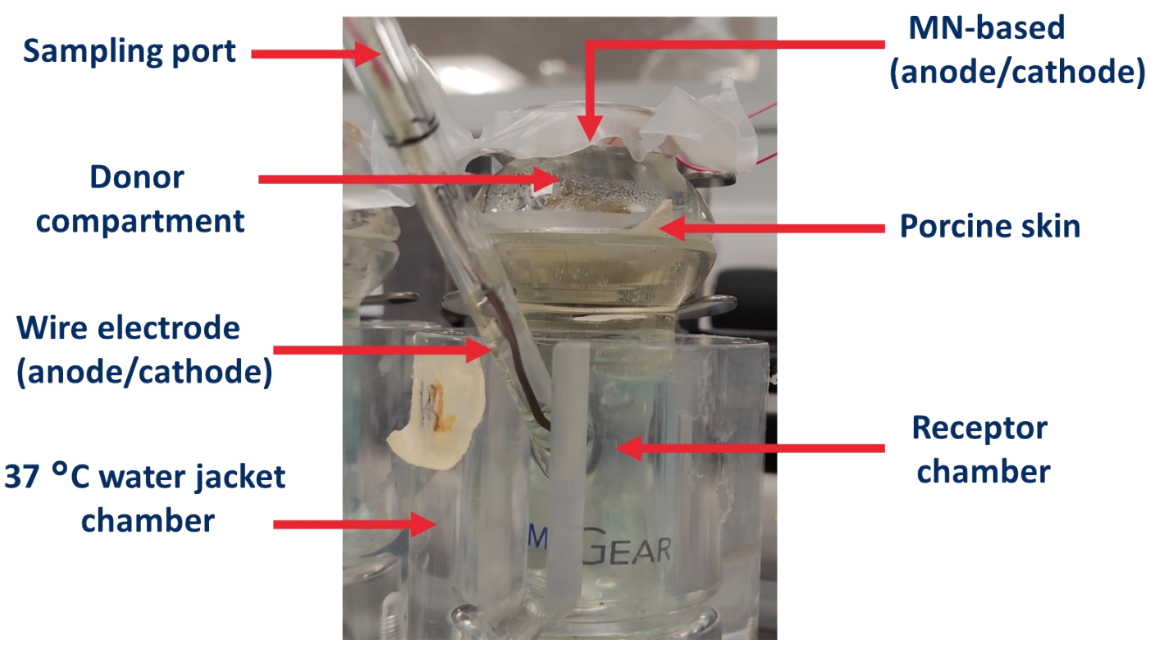

Fig. S9. Image of the Franz diffusion cell setup. The HMNI device is inserted into the skin and positioned in the donor compartment.

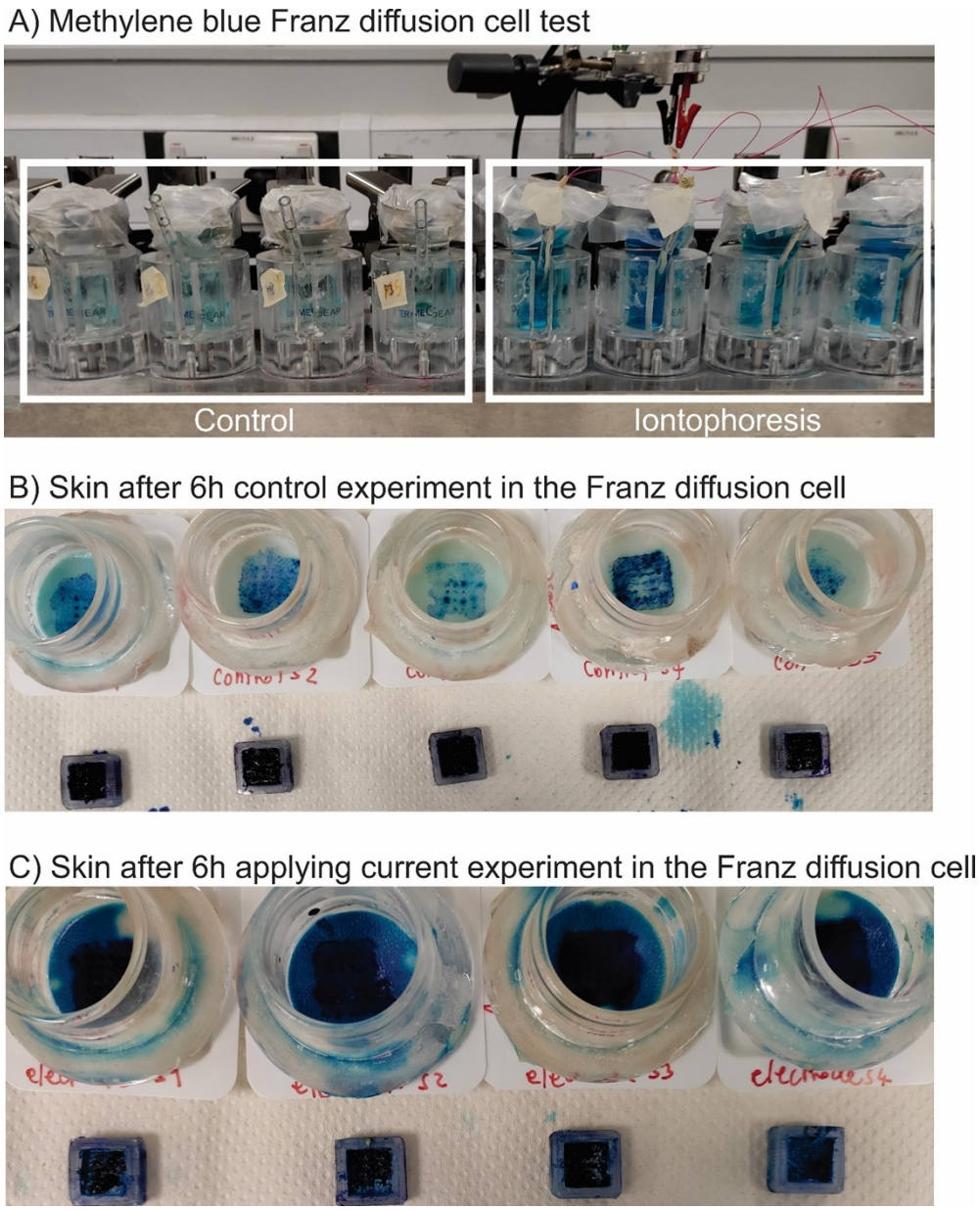

Fig S10. Images of the experiment with the IHMAS single electrode configuration: (A) IHMAS mounted on the Franz diffusion cell during the experiment, (B) Skin after 6 h under the control experiment (i.e. without applying current), and (C) Skin after 6h under the applied current experiment (i.e. 1 mA cm^{-2} per IHMAS device).

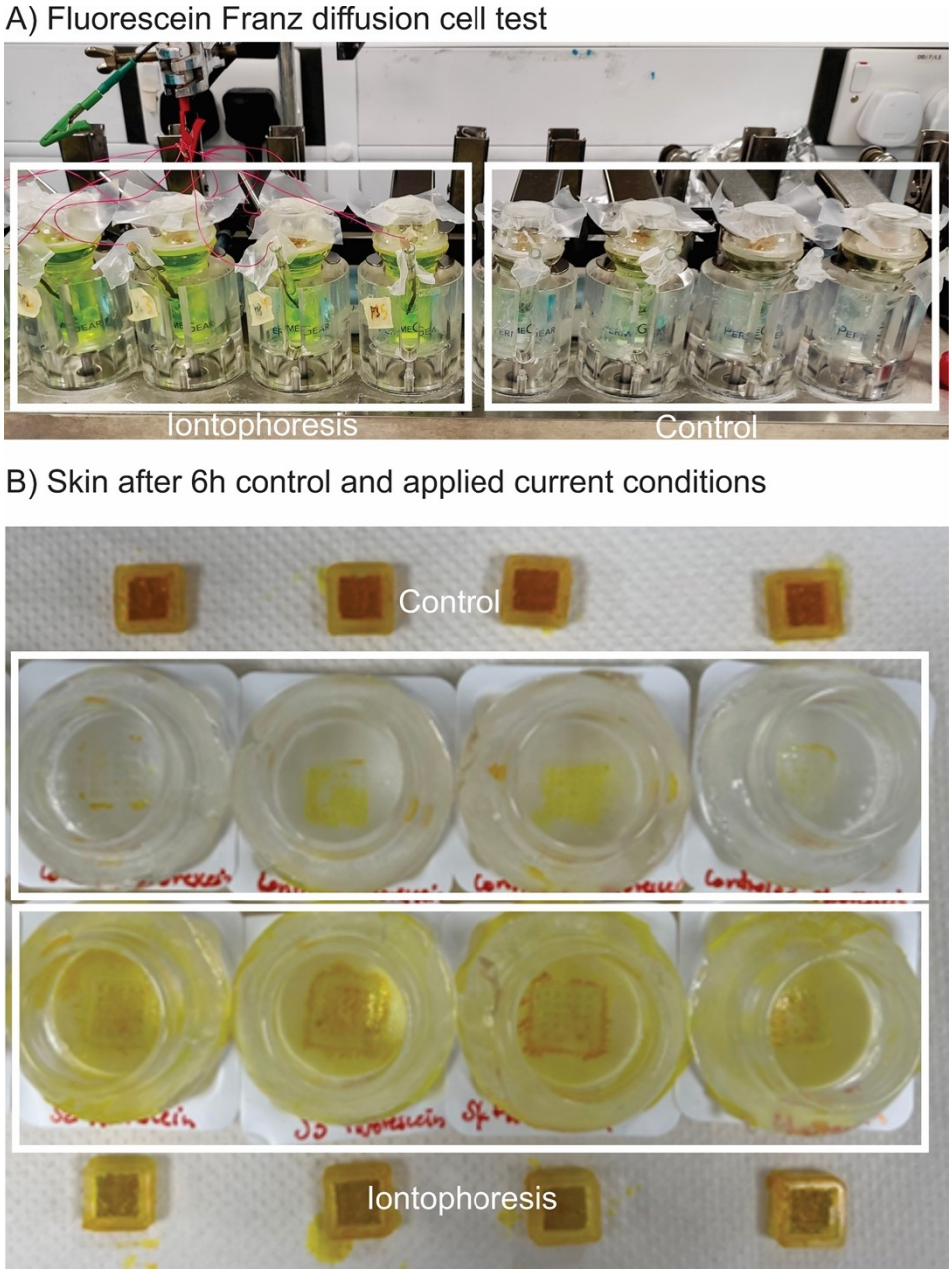

Fig S11. Images of the experiment with the IHMAS single electrode configuration mounted on the Franz diffusion cell for fluorescein sodium-loaded hydrogel: (A) Franz diffusion cell setup, and (B) skin after 6 h under the control and iontophoresis experiments (i.e. 1 mA cm^{-2} per IHMAS device).

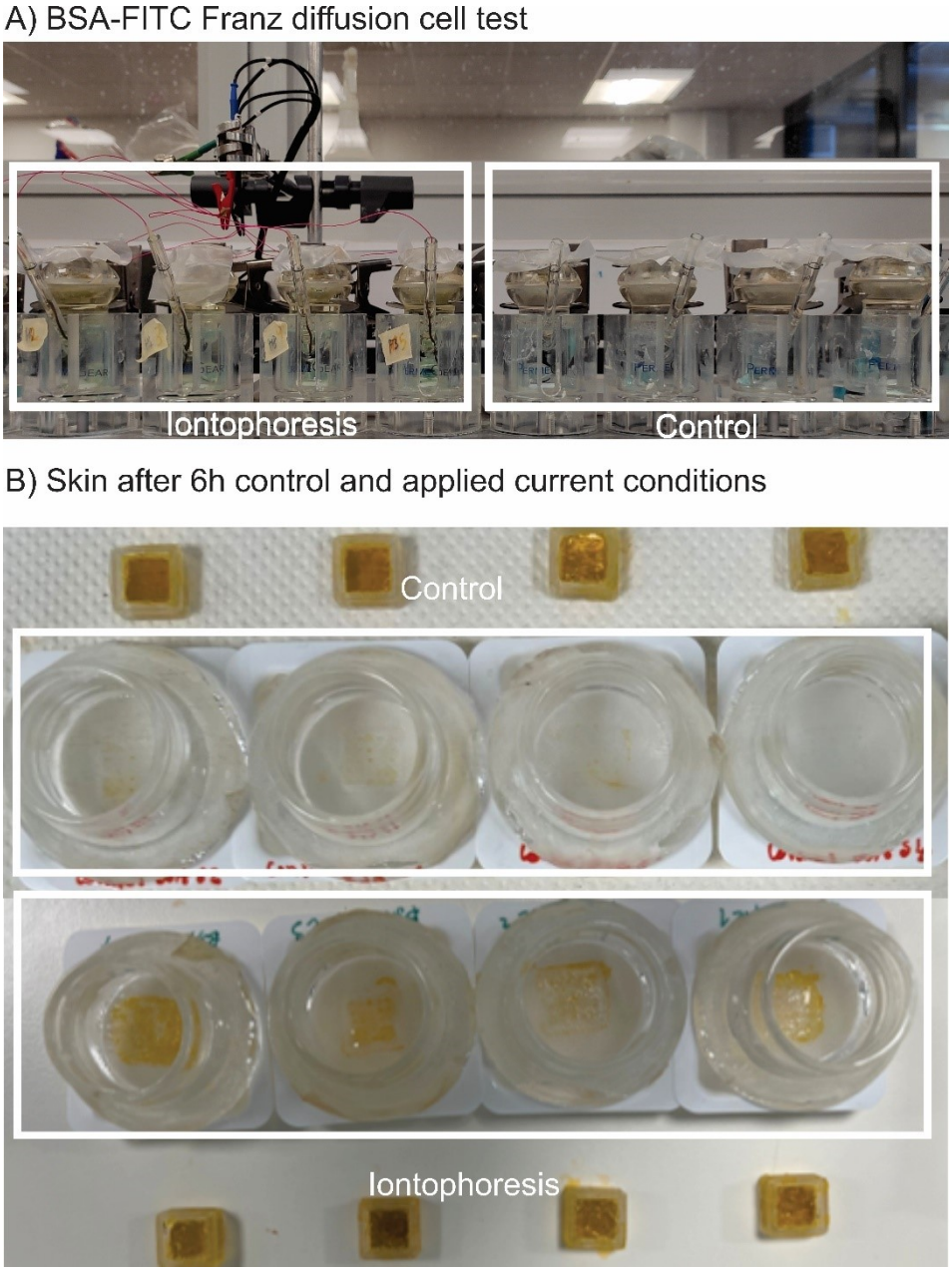

Fig S12. Images of the experiment with the IHMAS single electrode configuration mounted on the Franz diffusion cell for BSA-FITC hydrogel: (A) Franz diffusion cell setup, and (B) skin after 6 h under the control and iontophoresis experiments (i.e. 1 mA cm^{-2} per IHMAS device).

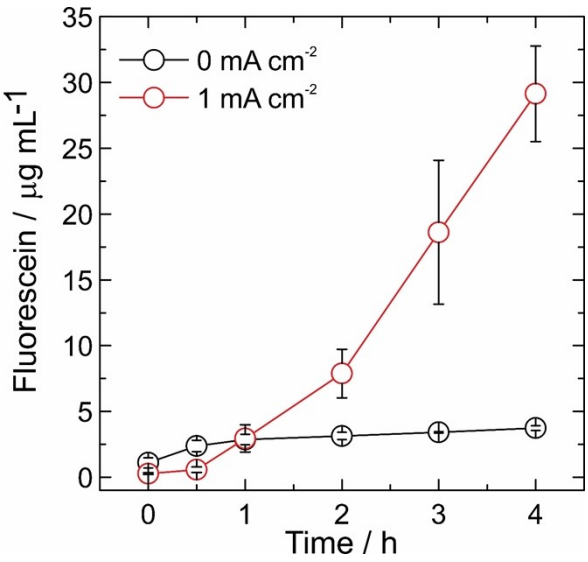

Fig. S13. *Ex vivo* test with fluorescein sodium-loaded hydrogel employing the integrated two-electrode iIHMAS system during 4 h in a Franz cell setup (means ± standard deviation, N = 2). The hydrogel was deposited in the cathode compartment.

References

1 E. Larrañeta, J. Moore, E. M. Vicente-Pérez, P. González-Vázquez, R. Lutton, A. D. Woolfson and R. F. Donnelly, *Int. J. Pharm.*, 2014, **472**, 65–73.